Spin polarized surface resonance bands in single layer Bi on Ge(111)

F. Bottegoni,[1] A. Calloni,[1] G. Bussetti,[1] A. Camera,[1] C. Zucchetti,[1] M. Finazzi,[1] L. Duó,[1] and F. Ciccacci[1]
LNESS-Dipartimento di Fisica, Politecnico di Milano,Piazza Leonardo da Vinci 32, 20133 Milano, Italy

(Dated: January 22, 2016)

The spin features of surface resonance bands in single layer Bi on Ge(111) are studied by means of spin- and angle-resolved photoemission spectroscopy and inverse photoemission spectroscopy. We characterize the occupied and empty surface states of Ge(111) and show that the deposition of one monolayer of Bi on Ge(111) leads to the appearance of spin-polarized surface resonance bands. In particular, the C_{3v} symmetry, which Bi adatoms adopt on Ge(111), allows for the presence of Rashba-like occupied and unoccupied electronic states around the $\overline{\mathrm{M}}$ point of the Bi surface Brillouin zone with a giant spin-orbit constant $|\alpha_{\mathrm{R}}| = (1.4 \pm 0.1)$ eV·Å.

Spin generation, transport and dynamics in heavy metals with a large spin-orbit interaction are key features laying at the cutting edge of spintronics[1,2]. Typically, such materials are non-magnetic, with electronic bands in the bulk being spin-degenerate as a consequence of time-reversal and spatial inversion symmetry. However, thanks to the large spin-orbit interaction, the structural inversion symmetry breaking at surfaces or interfaces of heavy metals[3–6] can introduce a significant Rashba term in the Hamiltonian[7,8] at particular points of the surface Brillouin zone (SBZ), leading to the removal of the Kramers degeneracy. Similar effects are also observed when non-magnetic heavy metals such as Bi are deposited as thin films over the surface of lighter metals[2,9]. In all these cases, a shared drawback consists in the presence of spin degenerate bands at the Fermi level (E_F), associated with either the metallic substrate or the bulk, which reduce the total spin polarization of conduction electrons, hindering possible spintronic applications.

In this context, the exploitation of a semiconductor substrate with an appropriate crystal symmetry seems to be very promising for electrical spin manipulation in non-magnetic heavy metals. Indeed, experiments and calculations indicate that the deposition of thin Bi films on Si(111)[10,11] and Ge(111)[12–15] surfaces leads to a giant Rashba-type spin-splitting[16]. The spin-polarized surface bands in these systems prevalently lie in the surface-projected gap of the semiconductor[10], thus preserving a very high spin polarization. However, a confirmation that these mechanisms indeed result in fully spin-polarized bands is still missing. Notably, a Rashba-like spin texture has been observed in unoccupied surface resonance bands of Tl/Si(111)[17].

The Rashba spin-orbit Hamiltonian derived from a nonrelativistic approximation of the Dirac equation can be expressed as[18]:

$$\widehat{H}_R = \frac{\hbar^2}{4m_0^2c^2}\left(\frac{\partial V}{\partial z}\mathbf{u}_z \times \widehat{\mathbf{p}}_{\parallel}\right)\cdot\widehat{\boldsymbol{\sigma}}, \qquad (1)$$

where m_0 and c are the free electron mass and the speed of light, respectively, V is the potential, z the axis perpendicular to the surface, $\mathbf{u}_z$ the unit vector parallel to z, $\widehat{\mathbf{p}}_{\parallel} = \hbar\widehat{\mathbf{k}}_{\parallel} = \hbar(\widehat{k}_x, \widehat{k}_y)$ is the in-plane momentum operator, and $\widehat{\boldsymbol{\sigma}}$ stands for the spin operator. In the frame of a nearly-free electron (NFE) model for an electron gas in the (x, y) plane, the surface state wave function can be written as $\psi(\mathbf{r}) = e^{i\mathbf{k}_{\parallel}\cdot\mathbf{r}_{\parallel}}\phi(z)$, where $\mathbf{k}_{\parallel} = (k_{\mathrm{x}}, k_{\mathrm{y}})$, $\mathbf{r}_{\parallel} = (x, y)$ and $\phi(z)$ describes the z-dependence of the wave function. In this case, the first-order correction to the energy spectrum, given by the spin-orbit Hamiltonian, is $\Delta E_{\mathrm{R}} = \langle\psi|H_{\mathrm{R}}|\psi\rangle = \alpha_{\mathrm{R}}|\mathbf{k}_{\parallel}|$, where $\alpha_{\mathrm{R}} \propto \int d\mathbf{r}\,|\phi(z)|^2\partial V/\partial z$ is the Rashba spin-orbit constant (Rashba parameter)[7,8]. For a single layer of heavy atoms on a semiconductor, $\partial V/\partial z$ is large only in the vicinity of the heavy adatoms and is therefore anti-symmetric across the plane containing the heavy nuclei, leading to $\alpha_{\mathrm{R}} \to 0$ if $\phi(z)$ has a well-defined parity with respect to such a plane. The substrate thus plays a relevant role in determining the magnitude of α_{R}[13], since it breaks the symmetry of the Bi overlayer and actively participates in determining the charge density distribution along the z-axis perpendicular to the surface.

In this paper, we investigate the spin properties of occupied and unoccupied surface resonance bands in one atomic layer (ML) of Bi grown on Ge(111), which represents one of the most promising materials for spintronic applications due to the large spin-orbit interaction and long spin relaxation times[19]. In particular, by means of angle- and spin-resolved ultraviolet photoemission spectroscopy we show that, for 1 ML Bi/Ge(111), the surface resonance bands around the $\overline{\mathrm{M}}$ point of the Bi SBZ are spin polarized due to the presence of a large Rashba term with $|\alpha_R| = (1.4 \pm 0.1)$ eV·Å. Moreover, angle- and spin-resolved inverse photoemission spectroscopy hints at a spin polarization of Bi-derived empty states around $\overline{\mathrm{M}}$, revealing that the Rashba character of the electronic states is maintained also above the Fermi level.

Bi was evaporated in ultra-high vacuum (base pressure in the low 10^{-8} Pa) from a BN crucible at a rate of about 1 Å/min, calibrated by means of a quartz crystal microbalance[20]. The Ge(111) substrate (Sb-doped, resistivity $\rho = 0.18$ Ω·cm) was cleaned by Ar^+ ion sputtering (1 kV at normal incidence) and thermal annealing (few minutes at 900 °C), repeated until a sharp $c(2\times8)$ pattern[21,22] was visible (see Fig. 1a) with low energy electron diffraction (LEED), as shown in Fig. 1c. The Ge doping concentration was chosen to have the Fermi level of the substrate close to the conduction band min-

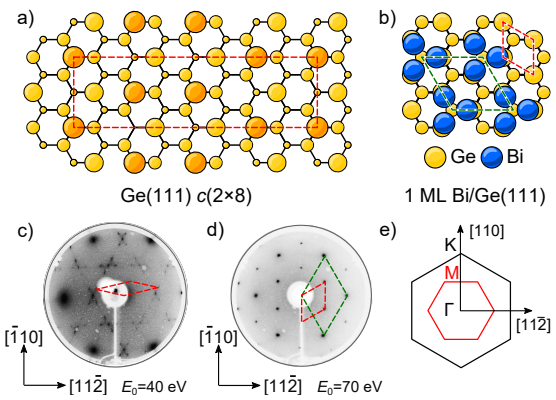

Figure 1. (Color online) Top views of the (a) Ge(111) $c(2\times 8)$ and (b) 1 ML Bi/Ge(111) reconstructions. Blue and yellow balls represent Bi and Ge atoms, respectively. LEED pattern of (c) Ge(111) $c(2\times 8)$ (electron beam energy $E_0 = 40$ eV) and (d) 1 ML Bi/Ge(111)-$\left(\sqrt{3}\times\sqrt{3}\right)R30°$ ($E_0 = 70$ eV) at $T = 300$ K, with the surface reciprocal-lattice vectors. (e) Surface Brillouin zones of Ge (black solid line) and Bi (red solid line).

imum, thus decreasing the superposition between the Bi surface states and the surface-projected Ge band structure. Bi was evaporated with the substrate kept at room temperature, with an estimated coverage slightly above 1 ML. The excess Bi atoms were then removed by heating the sample for 5 min at 450 ℃. Bi deposition and annealing resulted in a sharp LEED pattern, indicative of the presence of a $(\sqrt{3}\times\sqrt{3})R30°$ surface reconstruction (indicated in the following simply as $\sqrt{3}\times\sqrt{3}$), as shown in Fig. 1d. This diffraction pattern, which is characteristic for a Bi atomic layer on Ge[13], results from Bi atoms forming trimers (with C_{3v} symmetry), as shown in Fig. 1b. The deposition of further Bi layers led to the appearance of additional faint LEED spots attributed to the formation of Bi clusters with the bulk (rhombohedral) Bi crystal structure exposing the (110) face[23].

Valence band angle-resolved photoemission spectroscopy (ARPES) was performed with unpolarized He Iα radiation ($h\nu = 21.2$ eV). The photoelectrons were collected by a 150 mm hemispherical analyzer (from SPECS GmbH) equipped with a standard multichannel detector and a dedicated mini-Mott setup for spin-resolved (SR) ARPES measurements[24]. The FWHM energy (angular) resolution was about 40 meV (1°) and 150 meV (2°) for ARPES and SR-ARPES, respectively. Inverse photoemission (IPES) spectra were acquired in the isochromat mode: the impinging electron momentum and energy were controlled through the electron optics system, while the outgoing photons range were detected by a bandpass detector ($h\nu = 9.4$ eV) with FWHM energy and angular resolution of 600 meV and 3°, respectively[24–27].

All measurements were performed with the sample kept at 100 K. The electronic structure of 1 ML Bi/Ge(111) was mapped along the $\overline{\Gamma}\,\overline{\mathrm{M}}$ direction of the $(\sqrt{3}\times\sqrt{3})$ SBZ (see Fig. 1e) by tilting the Ge(111) substrate around the [11$\bar{2}$] direction. The experimental results obtained by spin-integrated ARPES are presented in Fig. 2. Following a standard procedure[13], the binding energy E_B dispersion of the main photoemission features was eventually obtained by considering the minima of the second derivative of the ARPES intensity, plotted as a function of the energy- and angle-dependent parallel component of the photoelectron wavevector ($\mathbf{k}_\parallel$). The sampled momentum space extends from $\overline{\Gamma}$ to $\overline{\mathrm{K}}$, i.e. up to the boundary of the first (1×1) Ge SBZ.

The S1, S2 and S3 states observed for E_B ranging from of 0.5 to 2.5 eV (see Fig. 2) are symmetric with respect to the $\overline{\mathrm{M}}$ point and are therefore related to the Bi layer. In analogy with similar band structures observed for 1 ML Bi grown on Si(111)[28], we attribute these features to bonding between Bi atoms (S1) and back bonding between Bi and Ge (S2 and S3).

The ARPES spectra covering the energy-momentum region containing the S1 states of 1 ML Bi/Ge(111) are evidenced in Fig. 3a. Electrons with $\mathbf{k}_\parallel$ corresponding to the $\overline{\mathrm{M}}$ point of the Bi SBZ are collected in the spectrum measured at 12°. The red and green bars indicate the spectral features corresponding with S1 states, as identified by considering the minima of the second derivative of the ARPES intensity. S1 states are clearly split in two symmetric branches (S1 and S1') crossing each other precisely at the $\overline{\mathrm{M}}$ point, about 0.9 eV below E_F (see Fig. 3b). The surface-projected Ge band structure (not shown) partially overlaps with the S1 branches, therefore the latter should be considered as surface resonance states.

The splitting of the S1 band in two branches is attributed to the Rashba-type spin-orbit interaction, which lifts the spin degeneracy[7,8]. In the frame of the NFE model and considering that the in-plane symmetry around the $\overline{\mathrm{M}}$ point of the SBZ is preserved[13], the Hamiltonian determining the S1 and S1' states can be expressed as $\widehat{H} = \widehat{H}_0 + \widehat{H}_R$, where $\widehat{H}_R$ has been defined in Eq. (1) and $\widehat{H}_0 = p_\parallel^2/2m^*$ is the kinetic NFE term with $\mathbf{p}_\parallel$ and m^* being the in-plane momentum and the effective electron mass. The corresponding eigenvalues are

$$E_\pm(k_\parallel) = \frac{\hbar^2\bar{k}^2}{2m^*} \pm \alpha_R\bar{k}, \qquad (2)$$

with $\bar{k} = k_\parallel - k_M$, k_M being the crystal wave-vector at the $\overline{\mathrm{M}}$ point of the Bi $(\sqrt{3}\times\sqrt{3})$ SBZ. The two eigenvalues in Eq. (2) correspond to two bands crossing at $\overline{\mathrm{M}}$.

A distinctive feature of the Rashba effect, stemming from the coupling between the electron spin and momentum, consists in the two branches being fully spin polarized with opposite polarizations. To demonstrate the Rashba-type nature of the investigated states, we performed SR-ARPES on the S1 and S1' branches, probing two different $k_\parallel$ points at opposite sides [± 0.1 Å^{-1}, ver-

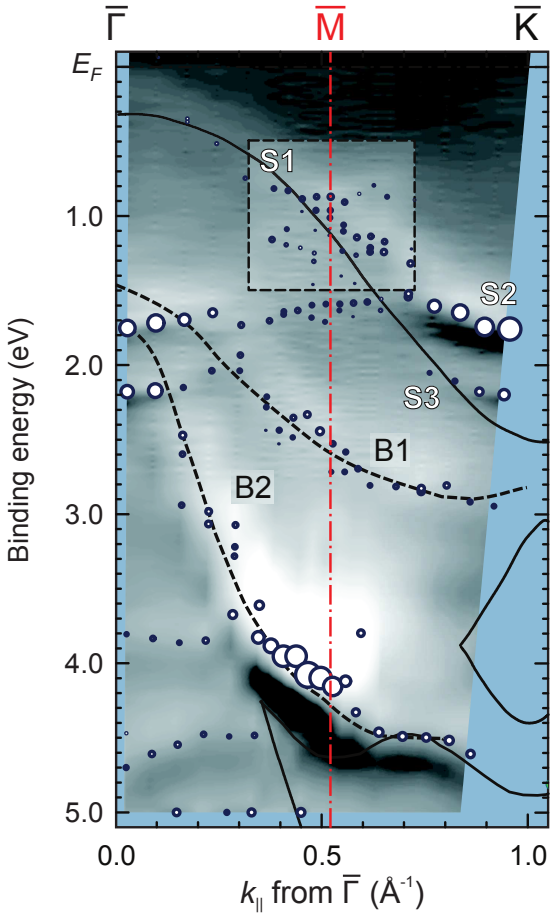

Figure 2. (Color online) Valence band ARPES measurements along the $\overline{\Gamma}\,\overline{K}$ direction of the first ($\sqrt{3} \times \sqrt{3}$) Bi SBZ for 1 ML Bi/Ge(111). The circles highlight the position of the photoemission features, whereas their dimension is related to the peak intensity of the second derivative of the spectrum. S1-3 indicate the surface resonance bands whereas B1 and B2 are bulk Ge states. The measurements were performed at 100 K.

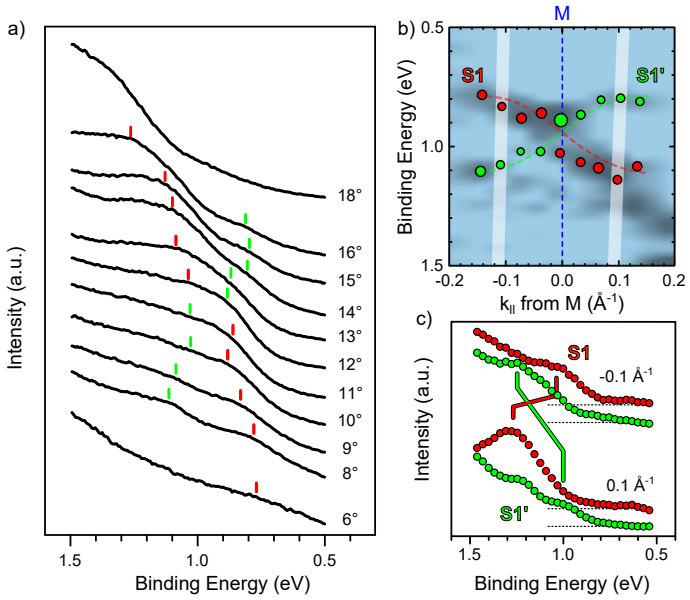

Figure 3. (Color online) (a,b) Evolution of the S1 and S1' branches around the $\overline{M}$ point (angular position around 12°) of the Bi SBZ: the spin-polarized states are represented by red and green bars in (a) and dots in (b), obtained by considering the minima of the second derivative of the ARPES intensity. (c) SP-ARPES on the S1 and S1' branches, probing two different k points at ± 0.1 Å^{-1} with respect to $\overline{M}$ (vertical white areas in Fig. 3b). The photoelectron polarization was detected along the $[11\bar{2}]$ direction of the Ge(111) substrate.

tical white areas in Fig. 3b] with respect to $\overline{M}$. The photoelectron spin polarization was detected in the direction perpendicular to the electron momentum along the $\overline{\Gamma}\,\overline{M}$ direction {parallel to the $[11\bar{2}]$ direction of the Ge(111) substrate}. Figure 3c shows the resulting spin-polarized spectra: consistently with the spin-integrated data presented in Fig. 2b, features about 0.8 eV and 1.1 eV below E_F are visible in each set of spectra. Their net spin polarization is reversed at opposite sides of $\overline{M}$ (S1 and S1' in Fig. 3c, marked with red and green circles, respectively). The spin polarization in the direction parallel to the electron momentum vanishes (within our experimental accuracy), confirming that the electron spin is perpendicular to the momentum, as expected according to the Hamiltonian of Eq. (1) for a Rashba-type interaction. The fact that the spin-polarized spectra of Fig. 2c are not perfectly symmetric with respect to the $\overline{M}$ point is due to the surface resonance nature of the S1 and S1' branches, which lye close to bulk Ge states that give different spectral contributions at opposite sides of $\overline{M}$.

By fitting the S1 and S1' branch dispersion of Fig. 3b with the relation of Eq. 2, it is possible to estimate the Rashba spin-orbit constant α_R and the in-plane electron effective mass m^*. For a rather narrow wave-vector interval of (± 0.2 Å^{-1}) around the $\overline{M}$ point we obtain $|\alpha_R| = (1.4 \pm 0.1)$ eV·Å and $m^* = (-0.8 \pm 0.1)m_0$, comparable with the values reported in Ref. 13. In this case, the wave-vector offset $k_0 = \alpha_R m^*/\hbar^2$, defined as the difference between the wave-vector related to the band maximum and $k_{||} = k_M$, and the Rashba spin-splitting $\Delta E_R = \hbar^2 k_0^2/2m^*$ are $k_0 = (0.14 \pm 0.02)$ Å^{-1} and $\Delta E_R = (-100 \pm 20)$ meV, respectively.

Figure 4 shows angular-resolved IPES spectra collected on Ge(111) and SR-IPES spectra collected on 1 ML Bi/Ge(111). The angular range straddles the $\overline{M}$ point (corresponding to the momentum of the electrons emitted at an angle of 22° with respect to the sample normal) of the 1 ML Bi/Ge(111) SBZ. The four spectra cover $k_{||}$ values between +0.15 and -0.15 Å^{-1}) with respect to $\overline{M}$ along the $\overline{\Gamma}\,\overline{\Gamma'}$ direction. The electron spin polarization for 1 ML Bi/Ge(111) was detected along the $[11\bar{2}]$ direction of the Ge(111) substrate, perpendicular to the $\overline{\Gamma}\,\overline{M}$ direction.

The non-dispersive broad peak around 2 eV above E_F

in the Ge(111) IPES spectra is attributed to a bulk Ge band, according to Straub *et al.*[29], whereas the small feature at 0.5 eV above E_F is related to unoccupied surface states. Spin-resolved AR-IPES experiments reveal that no spin-polarized features can be observed in the electronic structure of Ge(111) $c(2 \times 8)$.

After the deposition of 1 ML Bi, the Ge surface state at ≈ 0.5 eV above E_F is not detectable anymore, whereas a broad bulk peak at $\approx$ 2 eV above E_F is observed. Since such a feature is present also in the IPES spectra of Ge(111) $c(2 \times 8)$ (see Fig. 2b), we can conclude that the deposition of 1 ML Bi provides a new surface resonance in the unoccupied electronic states of the system. Notably, this feature shows a non-null spin polarization, which is reversed for angles corresponding to $\mathbf{k}_{\|}$ values at opposite sides of the $\overline{\mathrm{M}}$ point, suggesting that such a spectral feature retains the Rashba-like beahviour already observed for the surface states below E_F at $\overline{\mathrm{M}}$. However, the lack of theoretical calculations in this energy region and the energy resolution of the IPES technique, do not allow any further conclusion concerning the unoccupied electronic structure of 1 ML Bi/Ge(111).

In summary, we have investigated the spin and electronic properties of occupied and unoccupied surface resonance bands in 1 ML Bi grown on Ge(111). We have shown by means of spin- and angle resolved ultraviolet photoemission that the surface resonance bands around the $\overline{\mathrm{M}}$ point of the Bi SBZ are spin polarized due to the presence of a large Rashba term with $|\alpha_R| = (1.4 \pm 0.1)$ eV·Å. Moreover, we have also characterized the unoccupied surface resonance bands of the system through spin- and angle-resolved inverse photoemission spectroscopy, revealing that the Rashba character of the electronic states around $\overline{\mathrm{M}}$ is maintained also above the Fermi level.

The authors would like to thank G. Isella, A. Picone and E. Carpene for fruitful discussions. Partial funding is acknowledged to the project SEARCH-IV and SHAPES, granted by Cariplo foundation (grant n° 2013-0623 and 2013-0736, respectively).

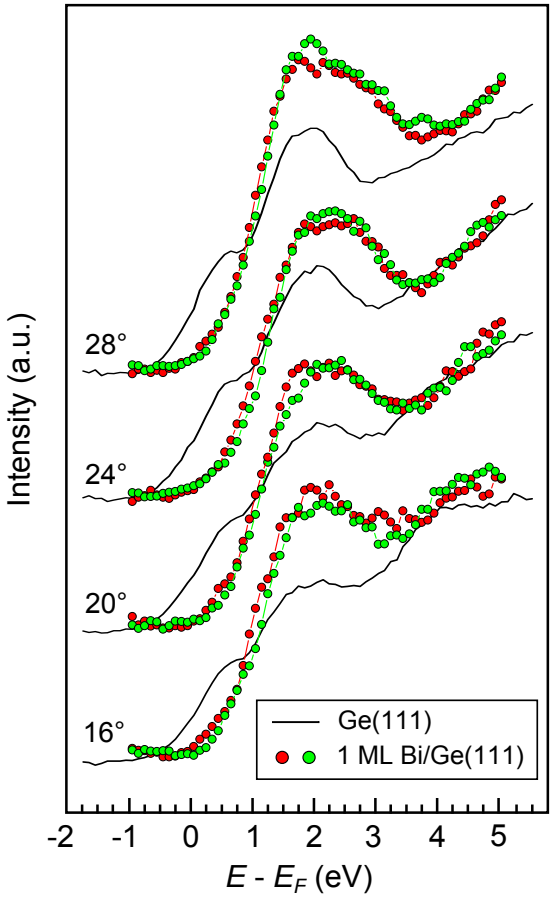

Figure 4. (Color online) IPES spectra of Ge(111) (lines) and SR-IPES spectra of 1 ML Bi/Ge(111) (green and red circles for majoriity and minority spins, respectively.). The investigated angular range straddles the $\overline{\mathrm{M}}$ (located around 22°) along the $\overline{\Gamma}\,\overline{\Gamma'}$ direction. The electron spin polarization for the SR-IPES spectra is detected in the perpendicular direction {parallel to the $[11\bar{2}]$ direction of the Ge(111) substrate}

REFERENCES

[1] T. Hirahara, T. Nagao, I. Matsuda, G. Bihlmayer, E. Chulkov, Y. Koroteev, P. Echenique, M. Saito, and S. Hasegawa, Phys. Rev. Lett. **97**, 146803 (2006).
[2] C. R. Ast, J. Henk, A. Ernst, L. Moreschini, M. C. Falub, D. Pacilé, P. Bruno, K. Kern, and M. Grioni, Phys. Rev. Lett. **98**, 186807 (2007).
[3] M. Hoesch, M. Muntwiler, V. N. Petrov, M. Hengsberger, L. Patthey, M. Shi, M. Falub, T. Greber, and J. Osterwalder, Phys. Rev. B **69**, 241401 (2004).
[4] A. M. Shikin, A. Varykhalov, G. V. Prudnikova, D. Usachov, V. K. Adamchuk, Y. Yamada, J. D. Riley, and O. Rader, Phys. Rev. Lett. **100**, 057601 (2008).
[5] M. Nagano, A. Kodama, T. Shishidou, and T. Oguchi, J. Phys.-Condens. Matter **21**, 064239 (2009).
[6] M. Hortamani and R. Wiesendanger, Phys. Rev. B **86**, 235437 (2012).
[7] E. I. Rashba, Sov. Phys. Solid State **2**, 1109 (1960).
[8] Y. A. Bychkov and E. I. Rashba, JETP Lett. **39**, 78 (1984).
[9] K. He, T. Hirahara, T. Okuda, S. Hasegawa, A. Kakizaki, and I. Matsuda, Phys. Rev. Lett. **101**, 107604 (2008).
[10] I. Gierz, T. Suzuki, E. Frantzeskakis, S. Pons, S. Ostanin, A. Ernst, J. Henk, M. Grioni, K. Kern, and C. R. Ast, Phys. Rev. Lett. **103**, 046803 (2009), 0905.0790.
[11] E. Frantzeskakis, S. Pons, and M. Grioni, Phys. Rev. B **82**, 085440 (2010).
[12] S. Hatta, C. Kato, N. Tsuboi, S. Takahashi, H. Okuyama, T. Aruga, A. Harasawa, T. Okuda, and T. Kinoshita, Phys. Rev. B **76**, 075427 (2007).
[13] S. Hatta, T. Aruga, Y. Ohtsubo, and H. Okuyama, Phys. Rev. B **80**, 113309 (2009).
[14] Y. Ohtsubo, S. Hatta, K. Yaji, H. Okuyama,

K. Miyamoto, T. Okuda, A. Kimura, H. Namatame, M. Taniguchi, and T. Aruga, Phys. Rev. B **82**, 1 (2010).
[15]Y. Ohtsubo, K. Yaji, S. Hatta, H. Okuyama, and T. Aruga, Phys. Rev. B **88**, 1 (2013).
[16]Y. M. Koroteev, G. Bihlmayer, J. E. Gayone, E. V. Chulkov, S. Blügel, P. M. Echenique, and P. Hofmann, Phys. Rev. Lett. **93**, 046403 (2004), 0404461 [cond-mat].
[17]S. D. Stolwijk, K. Sakamoto, A. B. Schmidt, P. Krüger, and M. Donath, Phys. Rev. B **90**, 161109 (2014).
[18]J. J. Sakurai, ed., *Advanced Quantum Mechanics* (Addison-Wesley, Reading, MA, 1967).
[19]F. Bottegoni, M. Celebrano, M. Bollani, P. Biagioni, G. Isella, F. Ciccacci, and M. Finazzi, Nat. Mater. **13**, 790 (2014).
[20]We estimate a Bi film thickness uncertainty of 20% from x-ray photoemission spectra, which show the expected evolution of the photoemission intensities as a function of the Bi coverage. Note that the 1 ML Bi coverage was obtained with the procedure of Ref. 13, which is independent from the microbalance calibration.
[21]R. D. Bringans and H. Höchst, Phys. Rev. B **25**, 1081 (1982).
[22]B. J. Knapp and J. G. Tobin, Phys. Rev. B **37**, 8656 (1988).
[23]S. Hatta, Y. Ohtsubo, S. Miyamoto, H. Okuyama, and T. Aruga, "Epitaxial growth of Bi thin films on Ge(111)," (2009).
[24]G. Berti, A. Calloni, A. Brambilla, G. Bussetti, L. Duò, and F. Ciccacci, Rev. Sci. Instrum. **85**, 073901 (2014).
[25]F. Ciccacci, E. Vescovo, G. Chiaia, S. De Rossi, and M. Tosca, Rev. Sci. Instrum. **63**, 3333 (1992).
[26]G. Chiaia, S. De Rossi, L. Mazzolari, and F. Ciccacci, Phys. Rev. B **48**, 11298 (1993).
[27]F. Ciccacci, S. D. Rossi, A. Taglia, and S. Crampin, J. Phys.-Condes. Matter **6**, 7227 (1994).
[28]K. Sakamoto, H. Kakuta, K. Sugawara, K. Miyamoto, A. Kimura, T. Kuzumaki, N. Ueno, E. Annese, J. Fujii, A. Kodama, T. Shishidou, H. Namatame, M. Taniguchi, T. Sato, T. Takahashi, and T. Oguchi, Phys. Rev. Lett. **103**, 156801 (2009).
[29]D. Straub, L. Ley, and F. J. Himpsel, Phys. Rev. B **33**, 2607 (1986).